JOURNAL OF MATERIALS SCIENCE **34** (1999) 115–122

Mechanism of combustion synthesis of TiC–Fe cermet

QUNCHENG FAN, HUIFEN CHAI, ZHIHAO JIN
State Key Laboratory for Mechanical Behavior of Materials, Xi'an Jiaotong University, Xi'an 710049, People's Republic of China

To investigate the mechanism of combustion synthesis of TiC–Fe cermet, a mixture of (Ti + C) + 30 wt % Fe was used for a combustion front quenching test, and the microstructural evolution in the quenched sample was analyzed by scanning electron microscopy and energy dispersive spectrometry. The temperature-time profile of the combustion was measured, and the phase constituents of the product were inspected by X-ray diffraction. Based on these results, the mechanism of the combustion synthesis was analyzed, and a ternary-reaction-diffusion/solution-precipitation model was proposed. Asynchronism and incompleteness of the combustion are discussed also.

1. Introduction

TiC–Fe cermet draws much attention because of its extremely high hardness and toughness attributes. It can be annealed and worked by normal machining techniques and can also be hardened by subsequent heat treatments.

In the past, TiC–Fe cermet was prepared by liquid-phase sintering of TiC and Fe powders. Recently, a combustion synthesis of TiC–Fe cermet from Ti, C, and Fe powders was studied by some researchers [1, 2] because this method has many advantages, such as simple equipment, an easily performed process, low energy consumption, non-polluting traits, etc. However, the mechanism of the combustion synthesis is not well understood.

As a typical system for self-propagating high-temperature synthesis (SHS), the Ti–C system has been studied extensively. The investigations involved are: calculations on the adiabatic temperature to show the effects of stoichiometry, dilution, and initial temperature of the reactants [3]; evolution of gases in the combustion [3, 4]; effects of materials and processing parameters on the reaction kinetics [5]; influence of reactant characteristics on the microstructures of TiC [6]; effects of process and carbon morphology on the morphology of TiC, and the fabrication of fibrous TiC [7–10]; and fabrication of dense bulk compacts of TiC ceramics [10–12]. However, the mechanism of interaction between Ti and C has been studied very little. Deevi suggested that the synthesis of TiC consists of an initial diffusional reaction of liquid Ti and C at the combustion front and an additional reaction leading to completion during the cool-down period [13]. Dunmead *et al*. proposed that the formation of TiC by SHS occurs by two different mechanisms. At high temperatures (>2711 K), a solution and precipitation mechanism is postulated, while at low temperatures (<2711 K), a carburization mechanism is postulated [14]. Choi *et al*. [9] found that when a relatively thick carbon fiber precursor is used, a small portion of the unreacted carbon core is observed at the center of the fibrous TiC product. They suggested that this phenomenon may be explained by two possible mechanisms: the shrinking core model [4] or a solution/precipitation model. Knyazik *et al*. investigated the interaction of Ti with C by using electrothermal explosion (ETE). The results showed that over a wide parameter range, ignition of mixtures of titanium and graphite is related to titanium fusion. But, to explain the difference of the slopes of specimen temperature versus time curves, they assumed that the TiC synthesis reaction also occurs before Ti fusion by a diffusion reaction mechanism, and this assumption was confirmed by a microstructural observation of a pre-aged specimen [15]. Saidi *et al*. [2] also found that when titanium powder with a diameter in excess of 100 μm and carbon black were heated to a temperature as high as 1450 °C at a rate to 350 °C min^{-1}, the reaction did not self-propagate. However, both X-ray diffraction (XRD) analysis and an optical micrograph evidenced the formation of TiC by solid-state diffusion of carbon at the TiC/Ti interface.

Clearly, the above-mentioned results are based on the observations of the characteristics of combustion synthesis and of its products. Further study on the mechanism should observe the microstructural transitions in the combustion synthesis process, but both high combustion temperature and rate make the observation very difficult. If a sample that was combusting in a self-propagating mode were quenched, the initial, intermediate, and end reaction products would be frozen in the quenched sample. Thus, the microstructural evolution could be observed and analyzed by scanning electron microscopy (SEM) and energy dispersive spectrometry (EDS). The microstructural transition in

the gasless combustion of the Ti–C system has been observed by using this combustion front quenching method (CFQM) [16]. The result showed that the onset of the reaction coincides with the melting of titanium, and the Ti melt spreads over the surface of the carbon particles in a form of thin film. At the same time, a reaction takes place on the boundary between the carbon and the melt leading to the formation of rounded TiC particles within the liquid film. Later, a more detailed SEM observation of microstructural evolution in the combustion synthesis of TiC was carried out, and a shell-core model was established by Fan *et al*. [17] using CFQM. The results showed that the reaction begins with the solid-state reaction diffusion of C into titanium particles forming a thin solid shell of TiC surrounding the titanium particles. The carbon atoms then diffuse into the titanium core through the TiC shell, and the TiC grains gradually crystallize.

Incorporation of iron into the mixture of Ti and C causes a more complicated combustion reaction, so the reports on this aspect are scarce. Choi and Rhee found that the combustion reaction between Ti and C in the Ti–C–Fe system is prevailing, while the addition of Fe mainly serves as a diluent and binder. Incorporation of Fe changes the shape of the TiC grains from angular to spherical, in a form of isolated particles surrounded by Fe phase but not agglomerated ones. The size of the grain decreases with an increasing amount of Fe addition. Based on the activation energy from the Arrhenius plot, it was postulated that the TiC formation rate is controlled by carbon diffusion into the liquid mixture of Ti–Fe [1]. Also, by use of the thermal explosion mode, the combustion synthesis of TiC–Fe ceramic has been investigated [2]. It has been found that the ignition temperature is dictated by the eutectic temperature of the Fe–Ti system, and it has been suggested that iron acts as a moderator for the reaction and leads to a decrease of the combustion temperature. Using CFQM, Fan *et al*. recently studied the role of iron addition in the combustion synthesis of TiC–Fe cermet. Besides acting as a diluent and binder, Fe was a reaction source [18]. However, the mechanism of combustion synthesis of any of polynary system is not understood.

In the present work, the mechanism of combustion synthesis of TiC–Fe cermet was studied using GFQM. The microstructural evolution of the specimen with the quenched combustion front was observed and analyzed with SEM and EDS. The combustion temperature of the reaction was measured, and the phase constituents of the combustion-synthesized product was inspected by XRD. Based on these experimental results, the mechanism of the combustion synthesis was discussed and a model for the mechanism was established. Also, the reasons for causing asynchronism and incompleteness of the reaction was analyzed.

2. Experimental procedures

56 wt% titanium powder (135–154 μm in diameter), 14 wt% carbon black (0.033–0.079 μm in diameter) and 30 wt% iron powder (135–154 μm in diameter) were mixed thoroughly for the following tests.

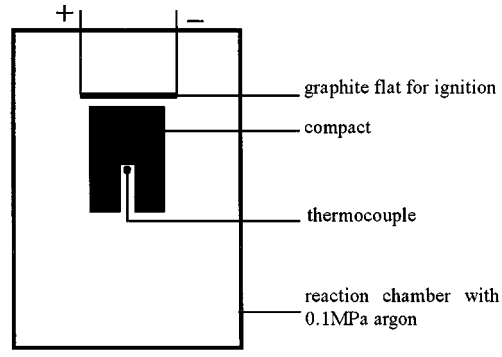

Figure 1 Schematic setting temperature-time profile during synthesis.

2.1. Measurement of temperature-time profile for combustion synthesis

The mixed powder was compressed to form a compact (14 mm in diameter and 18 mm in length) with a relative density of about 60%. A small hole (2 mm in diameter) was then drilled in the bottom of the compact, and a thermocouple pair of W-3%Re vs. W-25%Re (0.1 mm in diameter) was inserted into the hole and linked with an X–Y recorder, as shown in Fig. 1. The compact was ignited in a reaction chamber by an incandescent graphite flat placed 2 mm above the top surface of the compact at a pressure of 0.1 MPa of argon at an initial temperature of 298 K. This arrangement allowed recording of the temperature-time profile during the combustion synthesis process.

2.2. XRD inspection of combustion-synthesized product

The combustion product was ground into fine powder (<45 μm), and inspected by XRD (CoK_α) to study the phase constituents.

2.3. Combustion front quenching test

The mixed powder was compressed in a steel die, and a green compact (14 mm in diameter and 18 mm in length) was obtained with a relative density of about 60%. Part of the compact was pushed out of the die, with the remaining part being left in the die. The compact was ignited at its top surface in the reaction chamber, as shown in Fig. 2. Because of the cooling effect of the steel die, the combustion front had been quenched before it reached the bottom of the compact. The quenched

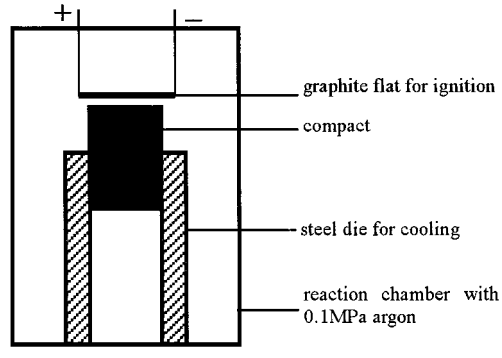

Figure 2 Schematic of the combustion front quenching test.

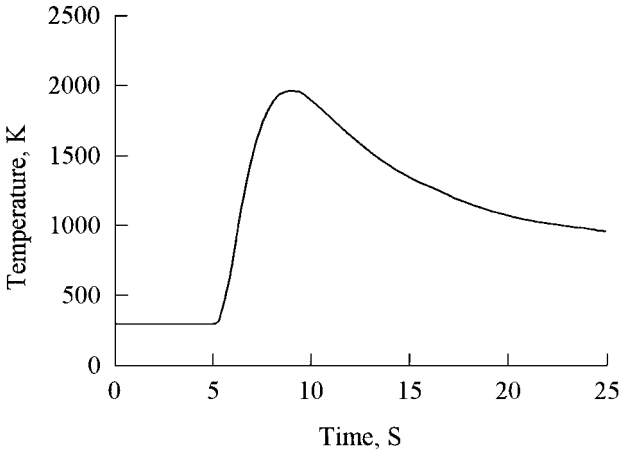

Figure 3 Temperature-time profile during combustion synthesis.

sample was then cut longitudinally for metallographic observation with SEM and EDS methods.

3. Experimental results

3.1. Temperature-time profile of the combustion synthesis

Fig. 3 shows the measured temperature-time profile of the combustion synthesis at a point of the combusting compact. An exothermic peak, with a temperature of 1926 K, is presented on the profile. This means the combustion temperature is below the melting point (1945 K) of titanium.

3.2. Phase constituent of combustion-synthesized product

The XRD pattern of the combustion-synthesized product in Fig. 4 shows that the product is composed of TiC, α-Fe, and a small amount of $TiFe_2$.

3.3. Microstructural evolution

Fig. 5 shows an SEM photograph of the initial reactants in the unreacted zone of the quenched specimen. EDS results showed that the bright particle "A" was Fe, and the grey ones, "B," were Ti, but the carbon black particles were too fine to be found.

3.3.1. Combustion reaction between Ti and C in Ti particle

Fig. 6 shows a reacting Ti particle. A clear change has occurred in the surface layer of the Ti particle, as shown

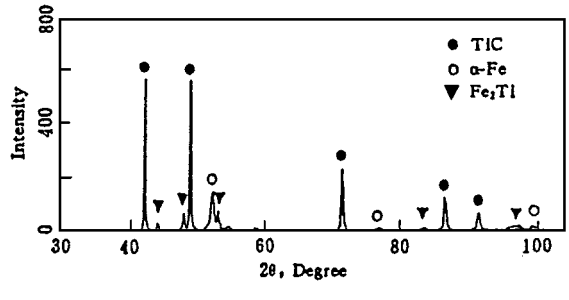

Figure 4 XRD pattern of the combustion-synthesized product.

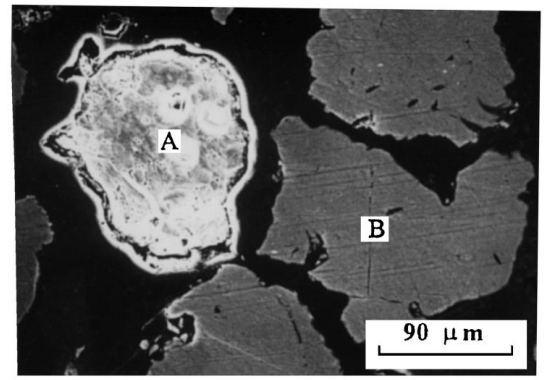

Figure 5 SEM of the initial reactants.

in Fig. 6a, and this change extends gradually toward its central region "C," as shown in Fig. 6b. Fig. 6c shows the structure of the region around the "C"/"D" interface in Fig. 6b. Fig. 6c indicates that many particles with an average diameter of about 1.0 μm have formed in the region "D," and they are separated by the binder phase. EDS results showed that these particles were TiC in which a small amount of Fe (Fe/Ti atom ratio of 6.50/93.50) was dissolved, and the binder phase was Ti-rich solid solution (Fe/Ti atom ratio of 18.90/81.10). The central region "C" was also Ti-rich solid solution, but the Fe content in it (Fe/Ti atom ratio of 4.50/95.50) was lower than that in the binder phase. Of course, carbon atoms must be involved in these phases. It is important to note that the shape and size of the reacting Ti particle, as shown in Fig. 6b, have not changed remarkably as compared with the initial Ti particle. Therefore, it may be suggested that the combustion reaction between Ti and C in the Ti particle takes place in the solid state, and the reaction starts from its surface layer and propagates to its core gradually to form TiC particles and a Ti-rich solid solution as a binder. Increase of Fe content in the binder phase led to the decrease of the melting point of the binder. The binder then melted and flowed with the TiC particles as the temperature was increased, as the region "E" in Fig. 6d. It must be noted, however, the reaction between Ti and C has not occurred in the Fe particle "F" by the side of the region "E" (Fig. 6d) where the reaction has occurred. This implies that the reactions between Ti and C take place in Ti and Fe particles separately, and the reaction in Fe is later than that in Ti particle.

3.3.2. Combustion reaction between Ti and C in the Fe particle

Fig. 7a shows an Fe particle in which change only appears in its surface region such as region "G," and the composition of the region "G" is different than that of the central region "H" of the Fe particle. The region "H" contained fewer carbon and titanium atoms (4.34 at % C, 0.24 at % Ti and 95.42 at % Fe) than the "G" (12.18 at % C, 1.31 at % Ti and 86.51 at % Fe). The structure of region "H," as shown in Fig. 7b, is similar to the high-carbon martensite, but the structure of region "G," shown in Fig. 7c, consists of two phases, i.e., high-carbon martensite and rod-shaped carbide phase.

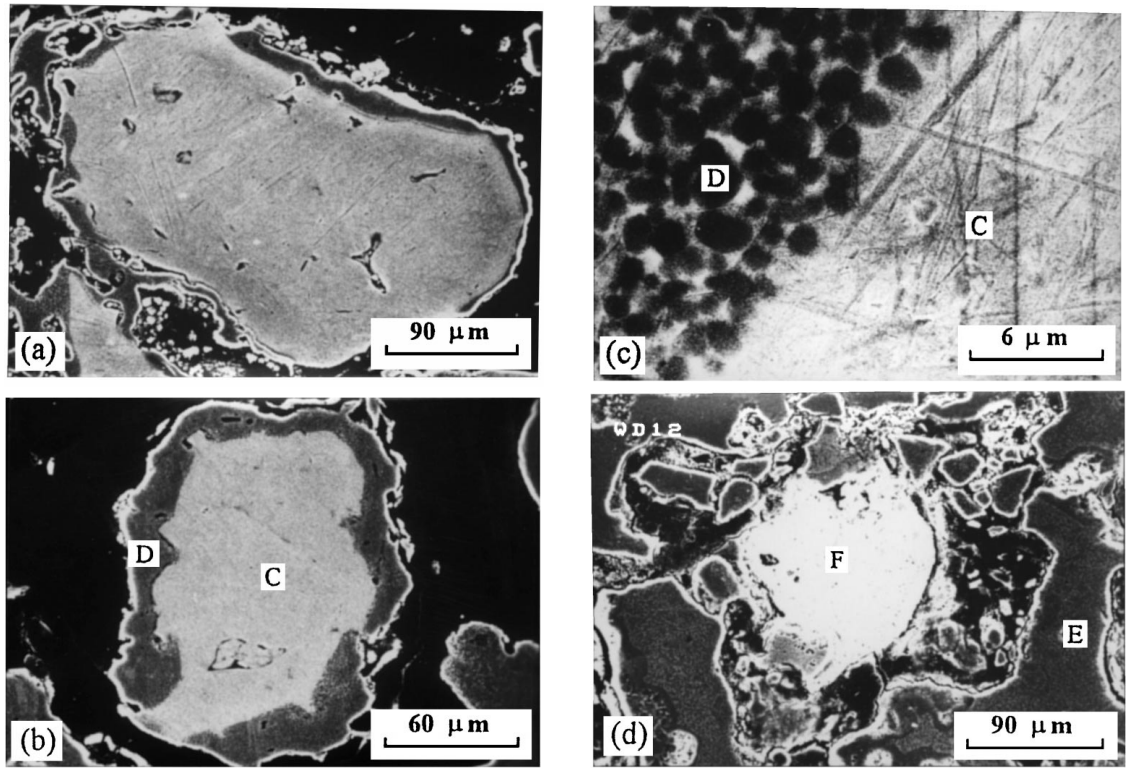

Figure 6 Reaction in Ti particle: (a) starting from the surface; (b) propagating toward the core; (c) reaction product; and (d) melting and flowing of the reacted Ti particle "E" and an unreacted Fe particle "F".

The carbide contained a large amount of C and a few Ti atoms (45.35 at % C, 0.38 at % Ti and 54.27 at % Fe); it seems to be an (Fe, Ti)C phase. From these results, it can be suggested that the change mainly results from diffusion of C into the Fe particle. With continuous diffusion of C into the central region, the melting point decreased, and the ledeburite (a eutectic structure in the Fe–C alloy, as indicated by an arrow) appeared in the Fe particle, as shown in Fig. 7d. The combustion reaction of Ti + C was then initiated in the surface region "I" of the molten Fe droplet and propagated gradually toward its central region "J," as shown in Fig. 7e. EDS showed that C, and especially Ti contents in the region "I" (5.00 at % C, 69.40 at % Ti and 25.60 at % Fe), were much higher than that in the region "J." (2.83 at % C, 5.09 at % Ti and 92.08 at % Fe). The structure of region "J," as shown in Fig. 7f, is not distinct from that in Fig. 7d, but the structure of region "I," as shown in Fig. 7g, is composed of TiC particles and an Fe-rich binder.

3.3.3. Fusing of molten Ti and Fe droplets

Fig. 8a shows the fusing of the molten Ti and Fe droplets. There are some bright regions, "K," and grey regions, "L." The structure of region "K" is shown in Fig. 8b; compared with Fig. 7f, it is not changed significantly. Consequently, it is an uncombusted region in Fe droplet. The region "L" is a combusted region, as shown in Fig. 8c, composed of TiC particles and binder.

3.3.4. Combustion-synthesized product

Fig. 9a shows the structure of the combustion-synthesized product. It is composed of cermet and many pores randomly distributed in various shapes. In the cermet, as shown in Fig. 9b, the TiC particles were basically spherical with an average diameter of about 2.5 μm and separated in the binder. EDS showed that a small amount of Fe atoms were dissolved in the TiC particles with an Fe/Ti atom ratio of 11.00/89.00, and Ti atoms dissolved in the binder with an Fe/Ti atom ratio of 88.30/11.70, so the binder was kept in the α-Fe lattice in the XRD pattern. In addition, there were some uncombusted regions in the product, as indicated by an arrow in Fig. 9a, of which the composition was 6.92 at % C, 21.12 at % Ti and 71.96 at % Fe and was corresponded to the Fe/Ti atom ratio of 77.31/22.69, with a structure shown in Fig. 9c. According to the Fe–Ti phase diagram [19], the bright phase in Fig. 9c is the $TiFe_2$ phase in the XRD pattern, and the grey structure easy to be etched may be the eutectic structure of $TiFe_2$ and α-Fe solid solution. This is associated with the incompleteness of the combustion synthesis.

4. Discussion

4.1. Mechanism of combustion synthesis

The combustion reaction of Ti + C is affected by many factors. On the one hand, it is influenced by the size of the titanium powder. Many results [8, 9, 16, 20] showed that the combustion process of the Ti–C system was preceded by the melting of Ti, when fine Ti powders were used; if Ti powder were coarse, the reaction began in the solid state as a shell-core model [17]. On the other hand, it is affected by the size of the carbon precursor. Deevi [13] found no self-sustaining combustion when the average particle sizes of Ti and C were 148 and 11 μm, respectively; the combustion wave only propagated a

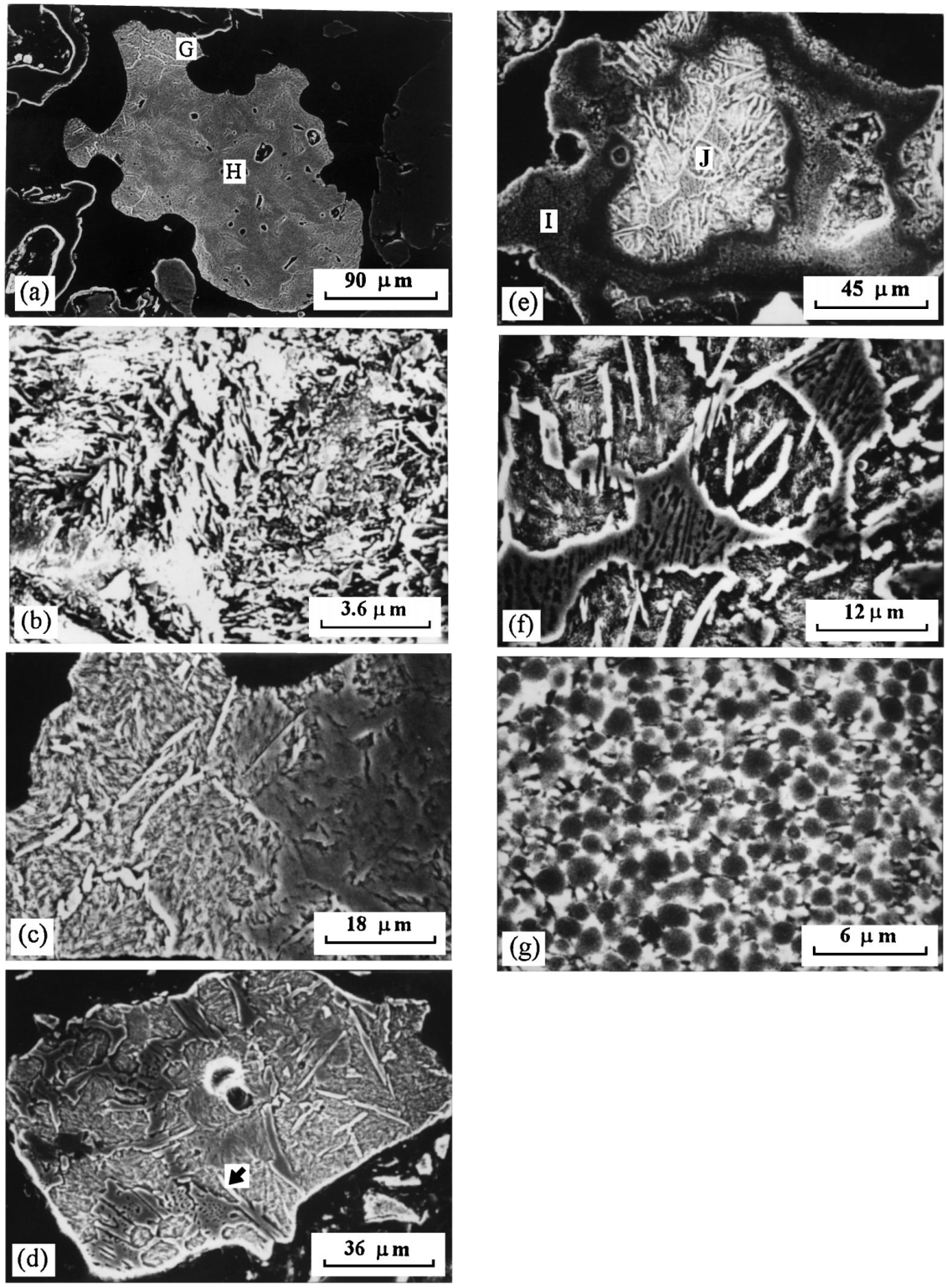

Figure 7 Reaction in Fe particle: (a) change starting from the surface region "G"; (b) structure of the region "H" in (a); (c) structure of the region "G" in (a); (d) Fe particle starting to melt; (e) the reaction starting from the surface region "I" and propagating toward the core region "J" of the molten Fe droplet; (f) structure of the region "J" in (e); and (g) structure of the region "I" in (e).

few mm. In contrast, Azatyan *et al*. reported (see also [13]) that titanium between 125 to 160 μm, 250 to 280 μm, and polydisperse with $\leq$280 μm (with carbon of $\leq$1 μm, argon pressure of 10 atm) underwent self-sustaining combustion. Moreover, in [17], although the size of Ti powder used was 135–154 μm in diameter, the carbon black was only 0.033–0.079 μm in diameter. Naturally the reaction mode of Ti + C would be affected by some other factors, so it is possible that the reaction takes place in the solid state under optimum conditions. In fact, the experimental results [13] showed that the ignition temperature, T_{ig}, of the Ti + C reaction was 1300 K at a starting temperature of 298 K, and the adiabatic temperature, T_{ad}, was 3210 K. The melting point of Ti (1945 K) is much higher than the T_{ig}, although it is much lower than the T_{ad}. This means that the reaction of Ti + C begins at least at 1300 K and takes place in the solid state between 1300–1945 K.

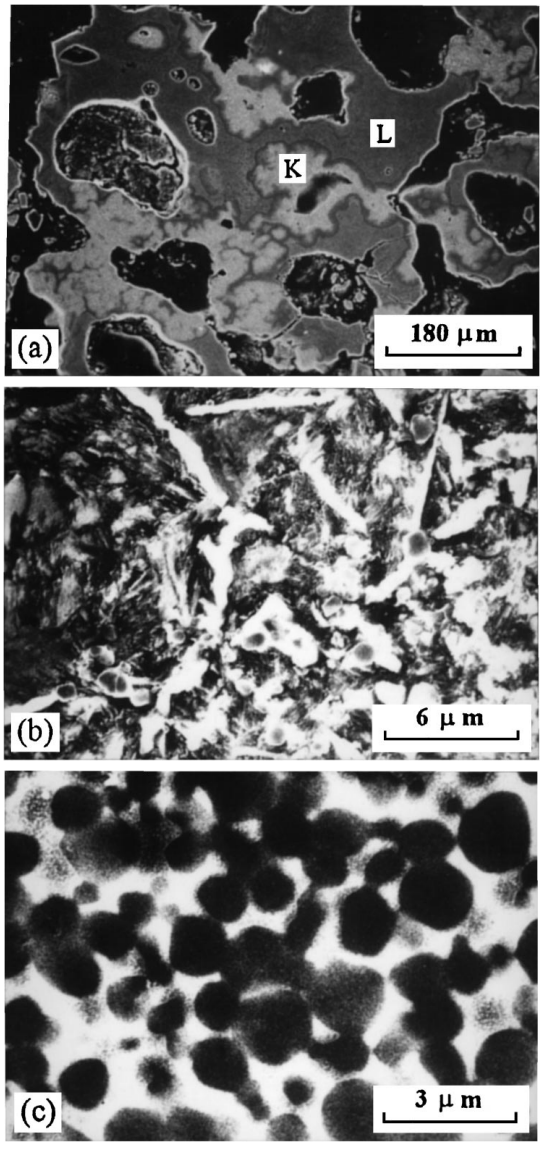

Figure 8 (a) Fusing of molten Fe and Ti droplets; (b) structure of the region "K" in (a); and (c) structure of the region "L" in (a).

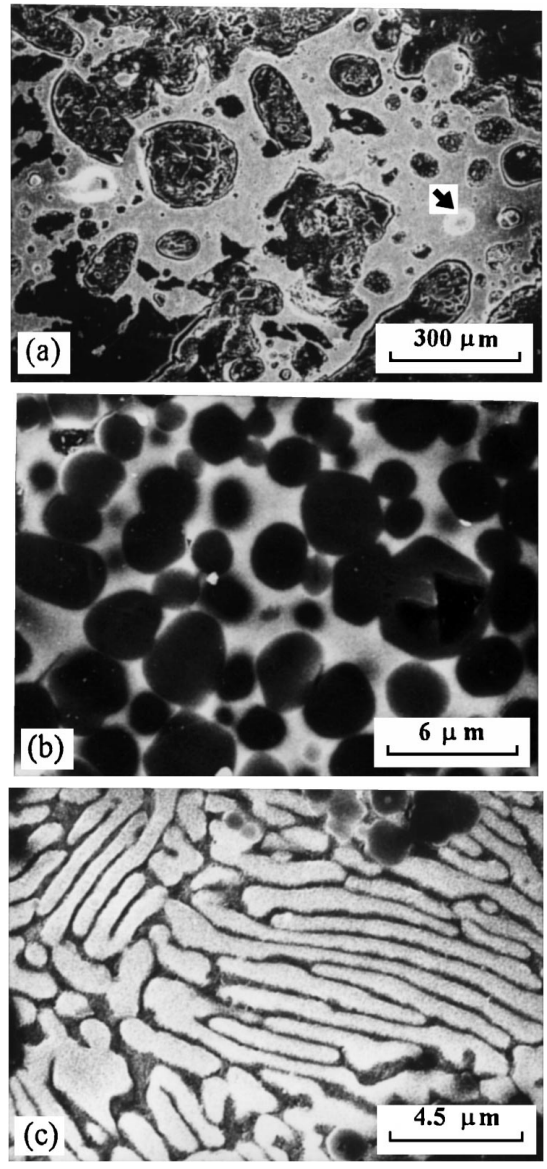

Figure 9 (a) Structure of the combustion-synthesized product showing TiC–Fe cermet, pores, and uncombusted regions indicated by an arrow; (b) structure of TiC–Fe cermet; and (c) structure of the uncombusted region.

When Fe powder is incorporated into the mixture of Ti + C, the combustion temperature is lower than that of the Ti–C system, and the more the Fe, the lower the observed combustion temperature [1]. The combustion temperature, T_c, measured in the present work is 1926 K, which is lower than that in [1] (2236 K) where finer titanium powder (average size of 30 μm) with 30 wt % Fe was incorporated. But the T_{ig} of about 1100 °C is not affected significantly by the incorporation of iron in a wide range of content [2]. Consequently, in this paper, it is reasonable to suggest that the reaction of Ti + C in the Ti particle occurs in the solid state. This can be explained as follows: First, the coarser the Ti powder, the lower the observed combustion temperature [21]; second, the coarser the Ti powder, the longer the distance of heat transfer from the surface to the core of Ti particle; third, the more Fe powder incorporated, the lower the observed combustion temperature [1]. Both long distance of heat transfer and low temperature do not benefit melting of the coarse Ti particle. In practice, shape and size of reacting Ti particle are not different from that of initial Ti particle, by comparing of Fig. 6b to Fig. 5. The only reaction mode of Ti + C in the solid state in the Ti particle is ternary-reaction-diffusion. The solid-state diffusion of C and Fe into Ti causes a Ti-rich solution; the TiC particles then precipitate out of the saturated solution from the surface of the Ti particle to the core. Because the diffusion rate of C in Ti is much higher than that of Fe in Ti, the initial product is composed of TiC particles and is Ti-rich rather than an Fe-rich solid solution. Afterwards, the solid solution melts and flows together with the TiC particles because the increase of Fe content in the Ti-rich solution leads to the decrease of its melting point.

The above-mentioned SEM results show that the reaction of Ti + C in the Fe particle is a process of the Fe particle melting and TiC precipitating in the molten Fe droplet. Diffusion of C into Fe particle leads to a decrease in the melting point of the Fe–C alloy and its melting, which accelerates dissolving of Ti into the molten Fe droplet. The reaction of Ti + C then starts from the surface and continuously propagates toward

the center, forming TiC particles and an Fe-rich binder when the concentration of C and Ti is saturated in the surface layer of the molten Fe droplet. Choi and Rhee [1] studied the effect of iron addition on TiC combustion synthesis. Based on the activation energy from the Arrhenius plot, they postulated that the TiC formation rate was controlled by carbon diffusion into the liquid mixture of Ti–Fe. Saidi *et al*. [2] developed a combustion model for the Fe–Ti–C system under a thermal explosion mode. They proposed that during the heating period, Ti and Fe powders reacted in the solid state to produce $FeTi_2$, which was a eutectic compound having a melting point of 1085 °C. At the ignition temperature, it almost matched the melting point of the Fe–Ti alloy; carbon dissolved in the molten droplets of $FeTi_2$, and the subsequent production of TiC released enough heat to initiate a self-sustaining reaction. Also, they examined this model by heating a pre-compacted mixture of Fe–Ti–C to 1100 °C and quenching the sample just before ignition. SEM inspection showed some liquid droplets around the Fe particles. However, the results of Choi and Rhee [1] showed that the XRD pattern for the sample heated mixture of Ti + Fe powders up to 1200 °C at a rate of 8 °C/min was composed of TiFe, $TiFe_2$, Ti, and Fe rather than $FeTi_2$. In this paper, both SEM and EDS results show that the melting of the Fe particle mainly results from the diffusion of C into the Fe particle, bringing the melting point of the Fe–C alloy down to 1148 °C, but not from the reaction of Fe and Ti forming $FeTi_2$. It is well known that the diffusion rate of C in Fe is much higher than that of Ti in Fe. Therefore, it is impossible that the $FeTi_2$ compound is formed by the solid-state reaction before C diffusing into Fe.

Although the Ti powder is the same size as the Fe powder used in this work, the Ti + C reaction in the Ti particle takes place mainly in the solid state, but the reaction in the Fe particle occurs mainly in the liquid state. This is because C diffusing into the Ti particle reaches the Ti–C eutectic temperature of 1654 °C ([3]), but the diffusion of C into the Fe particle leads to an Fe–C eutectic temperature of 1148 °C (see also the Fe–C phase diagram), i.e., the melting point of Ti–C is much higher than that of the Fe–C alloy.

With a temperature increase, the binder as an initial product in the Ti particle, i.e., the Ti-rich solid solution, melts and fuses with the reacting Fe droplet. The interdiffusion between Ti and Fe is accelerated by this fusing, and the activating combustion reaction in the molten Fe droplets and the transformation of the Ti-rich binder into the Fe-rich binder in the molten Ti droplets is enhanced.

4.2. Asynchronism of combustion synthesis

The SEM in Fig. 6d shows that the combustion synthesis is one of asynchronism, i.e., the combustion reaction of Ti + C takes place in the Ti and Fe particles, respectively; the reaction in the Ti particle is earlier than that in the Fe particle.

During the combustion synthesis, C and Fe atoms diffuse not only into the Ti particle, but also C and Ti atoms diffuse into Fe particle simultaneously; nevertheless, the reaction in the Ti particle is controlled by C diffusion, while in Fe particle it is controlled by diffusion of C as well as Ti. At the same temperature, C diffusing into Ti is much easier than that of C and Ti into Fe particle. First, the interstitial diffusion rate is higher than the substitutional diffusion one [22]. C into Ti and Fe diffusion is interstitial, but Ti into Fe is substitutional. Second, the diffusion rate in B.c.c. is higher than that in f.c.c. crystal [23]. Ti is B.c.c. at 882–1672 °C, but Fe is f.c.c. at 912–1394 °C. Therefore, the dissolving of a large amount of Ti into Fe occurs only the Fe particle being melted.

4.3. Incompleteness of combustion synthesis

Both the microstructure and the XRD pattern show that the combustion synthesis is incomplete because the residual phase, $TiFe_2$, is in the combustion-synthesized product. The residual phase is an Fe-rich compound, and it should be presented in the original Fe droplet. The incompleteness mainly results from coarse Ti and Fe particles. The coarser the Ti particle, the lower the observed combustion temperature [21], and the coarser the Fe particle, the longer the diffusion distance of C and Ti in the Fe particle. Both low temperature and long diffusion distance are not beneficial in saturating C and Ti at the center of Fe droplet so that the unsaturated Fe-rich crystalline is formed as $TiFe_2$, and a small amount of C was probably dissolved in it. Although the Ti powder is of the same size as the Fe powder in the present work, no residual phase is found at the center of the Ti particle because the diffusion rate into Ti is higher than that into the Fe particle. Also, Choi and Rhee [1] showed that the XRD pattern of the synthesized product from Ti/C (molar ratio) = 1.0 mixture with 30 wt % Fe mainly consisted of TiC and Fe phases with a small amount of Ti unreacted, where the sizes of titanium, graphite, and iron powders were 30 μm, 5 μm, and 2.5 μm, respectively. Perhaps fine reactants will eliminate incompleteness of combustion synthesis.

4.4. Model of combustion synthesis

To sum up, the mechanism of the TiC–Fe combustion synthesis can be described with a ternary-reaction-diffusion/solution-precipitation model. During combusion, the reaction of Ti + C takes place in the Ti and Fe particles, respectively, and the reaction in Ti is earlier than that in Fe particle. The reaction in the Ti particle occurs mainly in the solid state by ternary-reaction-diffusion of C and Fe into the Ti particle; it starts from the surface and propagates to the core of the Ti particle forming TiC and Ti-rich binder; the binder then melts and flows. But the reaction in the Fe particle occurs in the liquid state by dissolving C and Ti into Fe and precipitating TiC in the saturated Fe droplet. Diffusion of C into Fe causes decreasing of the melting point and leads to the melting of the Fe–C alloy, thus the dissolving of Ti into the molten Fe droplet is greatly accelerated. Precipitation of TiC starts from the surface

and propagates toward the core of the Fe droplet forming TiC particles and Fe-rich binder as it is saturated. Interdiffusion between Ti and Fe is promoted by the fusion of molten Fe and Ti droplets, thus the formed TiC–Fe cermet is composed of TiC particles and α-Fe binder. Obviously, the model will change with the size and mixture ratio of the reactants.

5. Conclusions

1. The combustion synthesis of TiC–Fe cermet is one of asynchronism, i.e., the reaction of Ti + C takes place in Ti and Fe particles, respectively. The reaction in Ti occurs earlier than that in Fe. This is because the diffusion rate of atoms into Ti is higher than that into the Fe particle.

2. The reaction in the Ti particle takes place in the solid state by ternary-reaction-diffusion of C and Fe into the Ti particle. It starts from the surface and propagates toward the core of the Ti particle, forming TiC particles and a Ti-rich binder.

3. Diffusion of C into Fe particle causes a decrease in melting point and accelerates the dissolving of Ti into the molten Fe droplet. When C and Ti are saturated, precipitation of TiC starts from the surface and propagates toward the core of the molten Fe droplet, forming TiC particles and Fe-rich binder.

4. With a temperature increase, the Ti-rich binder melts and fuses with the molten Fe droplet. It promotes the interdiffusion between Fe and Ti and the formation of the final product, TiC–Fe cermet.

5. The combustion synthesis may not be completed. Once coarse Fe and Ti powders are used, and because of the low diffusion rate in the Fe particle, a small amount of residual phase, $TiFe_2$, may exist in the combustion-synthesized product.

6. The mechanism of the combustion synthesis can be described with a ternary-reaction-diffusion/solution-precipitation model.

Acknowledgement

This research was supported by the Doctorate Foundation of Xi'an Jiaotong University.

References

1. Y. CHOI and S. W. RHEE, *J. Mater. Res.* **8** (1993) 3202.
2. A. SAIDI, A. CHRYSANTHOU, J. V. WOOD and J. L. F. KELLIE, *J. Mater. Sci.* **29** (1994) 4993.
3. J. B. HOLT and Z. A. MUNIR, *ibid.* **21** (1986) 251.
4. L. J. KECSKES and A. NIILER, *J. Am. Ceram. Soc.* **72** (1989) 655.
5. A. H. ADVANI, N. N. THADHANI, H. A. GREBE, R. HEAPS, C. COFFIN and T. KOTTKE, *J. Mater. Sci.* **27** (1992) 3309.
6. D. C. HALVERSON, K. H. EWALD and Z. A. MUNIR, *ibid.* **28** (1993) 4583.
7. Y. CHOI, M. E. MULLINS, K. WIJAYATILLEKE and J. K. LEE, *High Temp. Technol.* **8** (1990) 227.
8. M. E. MULLINS and E. RILEY, *J. Mater. Res.* **4** (1989) 408.
9. Y. CHOI, M. E. MULLINS, K. WIJAYATILLEKE and J. K. LEE, *Metall. Trans.* **23A** (1992) 2387.
10. S. ADACHI, T. WADA, T. MIHARA, Y. MIYAMOTO, M. KOIZUMI and O. YAMADA, *J. Am. Ceram. Soc.* **72** (1989) 805.
11. H. A. GREBE, A. ADVANI, N. N. THADHANI and T. KOTTKE, *Metall. Trans.* **23A** (1992) 2365.
12. O. YAMADA, Y. MIYAMOTO and M. KOIZUMI, *J. Am. Ceram. Soc.* **70** (1987) C-206.
13. S. C. DEEVI, *J. Mater. Sci.* **26** (1991) 2662.
14. S. D. DUNMEAD, D. W. READEY, C. E. SEMLER and J. B. HOLT, *J. Am. Ceram. Soc.* **72** (1989) 2318.
15. V. A. KNYAZIK, A. G. MERZHANOV, V. B. SOLOMONOV and A. S. SHTEINBERG, *Combust. Explos. Shock Waves* (English translation) **21** (1985) 333.
16. A. S. ROGACHEV, A. S. MUKAS'YAN and A. G. MERZHANOV, *Dokl. Phys. Chem.* (English translation) **297** (1987) 1240.
17. Q. C. FAN, H. F. CHAI and Z. H. JIN, *J. Mater. Sci.* **31** (1996) 2573.
18. *Idem.*, *ibid.* **32** (1997) 4319.
19. ASM, "Metals Handbook," 8th Ed., Vol. 8 (Metals Park, Ohio, 1973).
20. V. V. ALEKSANDROV, M. A. KORCHAGIN and V. V. BOLDYREV, *Dokl. Phys. Chem.* (English translation) **292** (1987) 114.
21. Z. A. MUNIR and U. A. TAMBURINI, *Mater. Sci. Rep.* **3** (1989) 277.
22. J. D. VERHOEVEN, "Fundamentals of Physical Metallurgy" (Wiley, NY, 1975).
23. A. G. GUY and J. J. HREN, "Elements of Physical Metallurgy" (Addison-Wesley, Reading, MA, 1974).

Received 23 October 1997
and accepted 16 July 1998